PHASE TRANSITIONS

Ferroelastic Phase Transitions in $(NH_4)_2TaF_7$

E. I. Pogorel'tsev[a], *, **S. V. Mel'nikova**[a], **A. V. Kartashev**[a, b], **M. S. Molokeev**[a],
M. V. Gorev[a, b], **I. N. Flerov**[a, b], and **N. M. Laptash**[c]

[a] *Kirensky Institute of Physics, Siberian Branch of the Russian Academy of Sciences,*
Akademgorodok 50—38, Krasnoyarsk, 660036 Russia
* *e-mail: pepel@iph.krasn.ru*
[b] *Institute of Engineering Physics and Radio Electronics, Siberian Federal University,*
ul. Kirenskogo 28, Krasnoyarsk, 660074 Russia
[c] *Institute of Chemistry, Far-Eastern Branch of the Russian Academy of Sciences,*
pr. Stoletiya Vladivostoka 159, Vladivostok, 690022 Russia
Received August 22, 2012

Abstract—The heat capacity, unit cell parameters, permittivity, optical properties, and thermal expansion of the $(NH_4)_2TaF_7$ compound with a seven-coordinated anion polyhedron have been measured. It has been found that the compound undergoes two successive phase transitions with the symmetry change: tetragonal ⟶ ($T_1 = 174$ K) orthorhombic ⟶ ($T_2 = 156$ K) tetragonal. The ferroelastic nature of structural transformations has been established, and their entropy and susceptibility to hydrostatic pressure have been determined.

DOI: 10.1134/S1063783413030232

1. INTRODUCTION

There are many chemical compounds with the crystal structure containing four-, six-, or seven-coordinated fluorine polyhedra, among which the most commonly occurring are fluorides with the general chemical formulas $AMeF_3$, $AMeF_4$, A_2MeF_4, A_3MeF_6, and $A_2A'MeF_6$, which have a perovskite-like crystal lattice [1–3]. The parent phases of these crystals are often have cubic or tetragonal symmetry, which can be lowered as a result of structural phase transitions associated, in particular, and, sometimes primarily, with rotations of the fluorine octahedra [MeF_6], while remaining almost undistorted. The mechanism of the phase transitions can be governed either by the processes of ordering of the octahedra, which in the parent phase have several crystallographically and energetically equivalent orientations, or by insignificant displacements of the fluorine atoms due to rotations of the octahedra through small angles. As a rule, structural transformations of this type have a ferroelastic nature [1–3].

In addition to the compounds with six-coordinated polyhedra, which have been intensively studied for a long time, there are fluorides of the general formula A_xMeF_7 ($x = 1, 2, 3$) with seven-coordinated anion polyhedra. By now, the number of known fluorides of this type is small and they have been studied rather superficially. The polyhedra [MeF_7], as a rule, can be represented as either a monocapped trigonal prism or a pentagonal bipyramid [4, 5]. Their symmetry and the valence of the central atom determine the degree

of disorder of the ligands and the symmetry of the crystal lattice as a whole. The A_3ZrF_7 (A = K, NH_4) compounds have cubic symmetry (space group $Fm-3m$, $Z = 4$) at room temperature [4, 5], whereas the symmetry of the $AMeF_7$ and A_2MeF_7 crystals also depends on the size of the cation A. It is known that, in the series of $ATaF_7$ (A = Ca, Ba, Sr, Pb) compounds, there can exist cubic and monoclinic structures [6], while the A_2TaF_7 compounds can have a tetragonal (A = Rb) [7] or monoclinic (A = K) crystal lattice [4].

The available information on the stability of the parent phases of A_xMeF_7 fluorides to variations in the external parameters has been reduced in the main only to the data on structural transformations due to reversible phase transitions [4, 7, 8]. There are no data on the physical properties of these compounds, which are necessary to determine the nature and mechanism of the phase transitions, to construct models of the crystal structure, and to determine the degree of disorder of individual structural elements.

In this work, we grew crystals of a fluoride compound with seven-coordinated anion polyhedra, namely, $(NH_4)_2TaF_7$, which was synthesized and described for the first time in 1866 [9]. We also investigated the heat capacity, unit cell parameters, permittivity, optical properties, and thermal expansion of this compound.
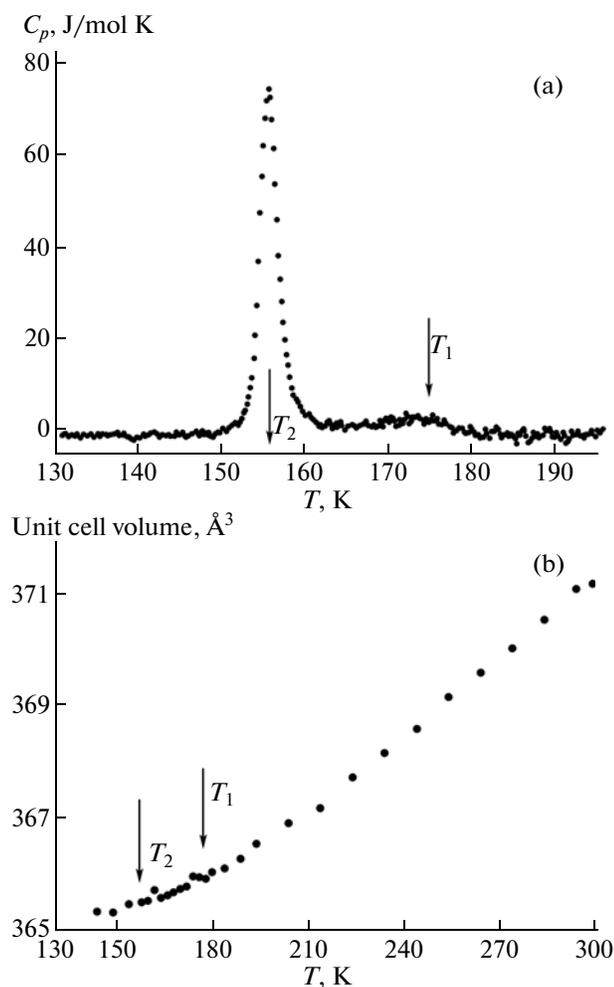
Fig. 1. Temperature dependences of (a) the excess heat capacity and (b) the unit cell volume of the $(NH_4)_2TaF_7$ compound.

2. SYNTHESIS, IDENTIFICATION OF SAMPLES, AND PRELIMINARY INVESTIGATIONS

Single crystals of $(NH_4)_2TaF_7$ were synthesized by two methods. The first method consisted in sintering the initial hydrated tantalum oxide (V) with the ammonium hydrodifluoride (NH_4HF_2) at temperatures in the range from 150 to 200°C according to the reaction

$$Ta_2O_5 + 7NH_4HF_2 = 2(NH_4)_2TaF_7 + 3NH_3 + 5H_2O.$$

The cake thus obtained was subjected to leaching of water with addition of a small amount of concentrated (40%) HF (all concentrations are given in mass %). The solution was filtered off and slowly evaporated in air until transparent single crystals of $(NH_4)_2TaF_7$ precipitated.

In the second case, during heating, the initial hydrated tantalum oxide $Ta_2O_5 \cdot nH_2O$ (15 g) interacted with concentrated (40%) HF (45 mL). A solu-

tion (20−25 mL) of concentrated ammonia (25%) was added to the filtered solution (the pH of the resulting solution was ~2). The formation of crystals of the studied complex occurred during a slow evaporation in air.

A careful chemical analysis for the fluorine content showed that the actual composition of the crystals corresponds to the formula $(NH_4)_2TaO_{0.3}F_{6.4}$. A similar partial isomorphic substitution of oxygen for fluorine was also observed in the related crystal Rb_2TaF_7 [7]. However, because the content of the impurity does not exceed ~4%, in the future we will use the stoichiometric formula $(NH_4)_2TaF_7$.

The identification of the grown crystals and the determination of their structural parameters were performed on a D8-ADVANCE X-ray diffractometer (CuK_α radiation, $\theta-2\theta$ scan mode). It was established that, at room temperature, the $(NH_4)_2TaF_7$ crystal has tetragonal symmetry (space group $P4/nmm$, $Z = 2$), as was previously found for the Rb_2TaF_7 fluoride, whose structure was investigated in [7]. In the X-ray diffraction patterns of the ammonium compound, we did not reveal reflections indicating the presence of foreign phases in the sample. The replacement of the spherical cation Rb^+ by the tetrahedral cation NH_4^+ led to a slight change in the unit cell parameters: $a = b = 5.8947(3)$ Å and $c = 10.6856(5)$ Å for $(NH_4)_2TaF_7$ and $a = b = 5.9118(3)$ Å and $c = 10.617(1)$ Å for Rb_2TaF_7.

The stability of the parent phase $(NH_4)_2TaF_7$ to variations in the temperature was investigated on a DSM-10M differential scanning microcalorimeter. The measurements were carried out in the temperature range from 110 to 350 K in the heating and cooling modes on a series of samples obtained from different crystallizations. The weight of the powder samples was ~0.10 g.

The preliminary calorimetric investigations revealed two anomalies in the heat capacity with maxima at the temperatures $T_1 = 174.3 \pm 2.0$ K and $T_2 = 154.5 \pm 1.0$ K, which were observed during the heating at a rate $dT/d\tau = 8$ K min^{-1} and reproduced during the thermal cycling. The temperature dependence of the excess heat capacity of the $(NH_4)_2TaF_7$ compound is shown in Fig. 1a. The anomaly observed at the temperature T_2 in the form of a sharp nearly symmetric peak with the maximum value $(\Delta C_p^{T2})_{max} \approx 70$ J (mol K)$^{-1}$ is characteristic of first-order phase transitions. This is also evidenced by the hysteresis of the phase transition temperature $\delta T_2 = 2.5$ K, which was revealed during the cooling of the sample. The anomaly observed at the temperature T_1 is significantly diffuse and amounts to only $(\Delta C_p^{T1})_{max}/(\Delta C_p^{T2})_{max} \sim 7\%$. A similar ratio between the enthalpies of the phase transformations was obtained by integrating the function $\Delta C_p(T)$: $\Delta H_1 \approx 25$ J mol^{-1} and $\Delta H_2 \approx 280$ J mol^{-1}. The small values of the thermal effects indicate slight distortions of the
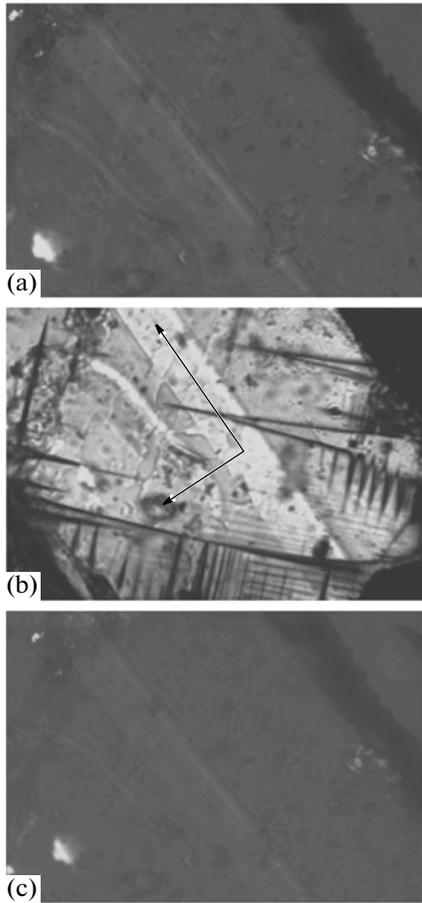
Fig. 2. Observation of the $(NH_4)_2TaF_7$ crystal plates of the (001)-cut in polarized light: (a) the G_1 phase, (b) twinning in the G_2 phase, and (c) the optically uniaxial phase G_3.

Fig. 3. Temperature dependences of the birefringence in the $(NH_4)_2TaF_7$ crystal: (*1a*, *1b*) birefringence Δn_c in the (001) plates of two crystallizations and (*2*) the main birefringence $\Delta n_a = n_o - n_e$.

structure due to the phase transitions. It seems likely that this is the reason why we did not reveal in the X-ray diffraction experiments significant differences between the X-ray diffraction patterns of the parent and low-temperature phases. This situation is no exception and has repeatedly been observed, for example, in the study of Rb_2KMeF_6 (Me = In, Sc) fluorides, which are also characterized by small enthalpy changes $\Delta H \approx 500$ J mol^{-1} [10]. In the X-ray experiments, phase transitions in these crystals were identified only from a change in the unit cell parameters. The temperature dependence of the unit cell volume of the $(NH_4)_2TaF_7$ compound is shown in Fig. 1b. In this case, too, we did not reveal significant anomalies associated with each of the phase transitions; however, as can be seen, it is in the region of transformations that the behavior of the function $V(T)$ drastically changes.

3. OPTICAL PROPERTIES

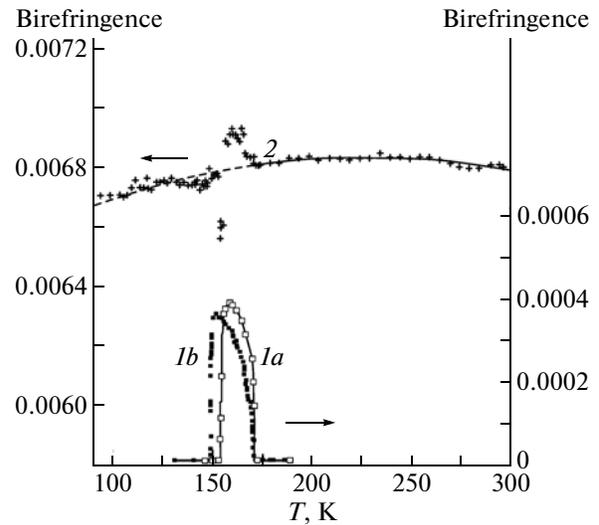Transparent crystals of $(NH_4)_2TaF_7$ predominantly had the form of rectangular (001) plates with the $(100)_T$ faceting. The polarization-optical investigations and birefringence measurements according to the Berek compensator method with an accuracy of ±0.0001 were performed on the (001) and (100) samples not subjected to preliminary treatment. The experiments were carried out with an "Axioskop-40" microscope and a "Linkam LTS 350" heating/cooling stage at temperatures in the range from 90 to 300 K.

The polarization-optical investigations showed that, at room temperature, the $(NH_4)_2TaF_7$ crystal is optically uniaxial (tetragonal). In the field of view of a polarizing microscope with crossed polarizers, we can see a dark sample of the (001)-cut (Fig. 2a) (the G_1 phase). During the cooling, as well as in the calorimetric experiments, we revealed two specific temperature points. Below $T_1 = 170.5$ K, the sample exhibits an optical anisotropy, and the wedge-shaped twins with boundaries along the [110] direction move in the sample with variations in the temperature (Fig. 2b). In this case, clearly extinctions of the crystal are observed along the $[100]_T$ direction (the G_2 phase). A further cooling leads to the fact that, at the temperature T_2, the optical anisotropy abruptly disappears, and the sample again becomes optically uniaxial (Fig. 2c) (the G_3 phase).

The temperature dependences of the birefringence in the $(NH_4)_2TaF_7$ crystal are shown in Fig. 3. Curves *1a* and *1b* describe the behavior of the optical anisotropy in the (001) plates of the samples obtained from two crystallizations. It can be seen from this figure that the birefringence Δn_c exists only in a narrow (~20 K) temperature range, which corresponds to the G_2 phase and has different widths for the samples prepared by the different method. In this case, the tem-
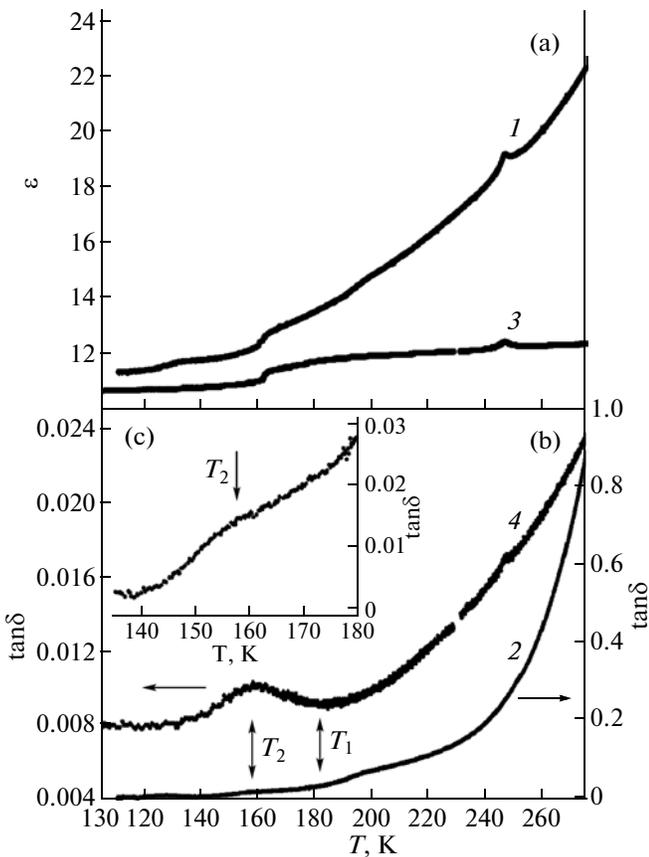
Fig. 4. Temperature dependences of the permittivity ε and the dielectric loss tangent $\tan\delta$ of the $(NH_4)_2TaF_7$ compound measured at frequencies of (*1, 2*) 1 kHz and (*3, 4*) 1 MHz: (a, b) over a wide temperature range and (c) in the temperature range of the phase transition $G_2 \longleftrightarrow G_3$.

perature T_1 is almost identical for both samples, whereas the temperature T_2 varies in the range 148.2–152.7 K and is characterized by an almost constant hysteresis $\delta T_2 \approx 0.4$ K.

Curve *2* in Fig. 3 shows the temperature dependence of the main birefringence $\Delta n_a = n_o - n_e$ of the $(NH_4)_2TaF_7$ tetragonal crystal. In the temperature range 170–300 K (the G_1 phase), all the experimental points are described by a second-order polynomial. The results the measurements of the dependence $\Delta n_a(T)$ in the G_3 phase fall on the same curve (with a small spread). In the region of the existence of the G_2 phase, there are rejections of the experimental points due to the appearance of the optical anisotropy of Δn_c and the mobility of twins.

Therefore, the results of the observations in polarized light of the $(NH_4)_2TaF_7$ crystal suggest the existence of the following sequence of changes in the symmetry of the phases: G_1 (*P4/nmm*) $\longleftrightarrow$ G_2 (*Pmmn*) $\longleftrightarrow$ G_3 (tetragonal). The orthorhombic primitive unit cell of the G_2 phase is chosen reasoning from the fact that, in this temperature range, the extinction in the (001)

samples is clearly pronounced and coincides with the axes of the tetragonal unit cell of the G_1 phase. The appeared twins with boundaries along the [110] direction in the G_2 phase indicate the loss of the corresponding symmetry elements.

Recall that the results presented in Fig. 3 were obtained on the untreated free growth plates. In the sample subjected to grinding and polishing before the optical experiment, there appeared inhomogeneous deformations, which are visible in the (001) plate as diffuse anisotropic spots. This sample is characterized by a downward shift in the temperatures of both transitions by 2–3 K.

4. DIELECTRIC PROPERTIES

Although the optical data indicate the absence of polar phases in $(NH_4)_2TaF_7$, we investigated the permittivity of the compound in order to elucidate the specific features of the phase transitions associated with the nature of these phases. Because of the presence of the ammonium cation in the structure of the tantalate, it was impossible to prepare a sample according to the classical ceramic technology. Therefore, the measurements were carried out on a pseudoceramic sample in the form of a pellet ($d = 8$ mm, $h = 2$ mm) prepared only by pressing without heat treatment. Silver electrodes were deposited by vacuum evaporation. The reliability of the results obtained for these samples was previously proved by comparing the data on the dependences $\varepsilon(T)$ measured on single-crystal plates and pseudoceramic samples of oxyfluorides [11].

The temperature dependences of the permittivity and dielectric loss tangent of the $(NH_4)_2TaF_7$ compound are shown in Fig. 4. It can be seen from this figure that a significant increase in both characteristics with variations in the temperature is observed at a measurement frequency of 1 kHz (curves *1, 2*). The most pronounced is the anomalous behavior of the permittivity in the form of a diffuse jump by ~0.4 units due to the phase transition at the temperature T_2 (Fig. 4a). In the region of the temperature T_1, the dependence $\varepsilon(T)$ does not exhibit specific features; however, there is an anomaly of the permittivity ε in the form of a peak at 246 K. The temperature dependence of $\tan\delta$ has a small mound-shaped anomaly only in the region of the phase transition at the temperature T_2 (Fig. 4c).

An increase in the measurement frequency to 1 MHz led to a sharp decrease in the rise of the permittivity and dielectric loss tangent with increasing temperature (curves *3, 4* in Figs. 4a, 4b). Most likely, this circumstance is associated with the fact that the experiments were carried out on a pseudoceramic sample not subjected to calcination at high temperatures, which could at least encourage a decrease in its density [11, 12]. At the same time, as in the case of the mea-

surement frequency $f = 1$ kHz, the abrupt change in the permittivity at the temperature T_2 is equal to ~0.4 units and the peak at a temperature of ~245 K remains unchanged (Fig. 4a). When the dielectric loss tangent is measured at a frequency of 1 MHz, the anomaly at the temperature T_2 is more pronounced, and the peak of $\tan\delta$ appears at 245 K, which was not observed in the experiments at the measurement frequency $f = 1$ kHz (Fig. 4b).

The behavior of the permittivity with small anomalies confirms the conclusion regarding the nonferroelectric nature of the phase transitions in $(NH_4)_2TaF_7$, which was drawn from the analysis of the optical properties.

5. HEAT CAPACITY

Detailed investigations of the heat capacity $\Delta C_p(T)$ of the $(NH_4)_2TaF_7$ crystal were carried out on an adiabatic calorimeter with three heat shields at temperatures in the range from 80 to 305 K. The calorimetric technique of the experiments performed in the discrete and continuous heating modes was similar to that described in [13]. The measurements were carried out on a sample weighing 0.230 g, which was prepared in the form of a cylindrical pellet ($d = 8$ mm) pressed from a powder obtained by grinding the single crystals. The sample was placed in an aluminum container with a heater. A good thermal contact between the sample and the container was ensured using the "Ramsay" vacuum grease.

The ratio of the heat capacities of the sample and fittings (container + vacuum grease) was 0.45/0.55. The error in the determination of the heat capacity did not exceed ±0.5%.

Figure 5a shows the temperature dependence of the molar heat capacity at constant pressure. This dependence exhibits anomalies in the temperature range which is consistent with the data obtained from the optical and preliminary calorimetric experiments. The phase transition temperatures determined from the maxima of the heat capacity measured under nearly equilibrium conditions at low heating rates of the sample $dT/d\tau = 3.5 \times 10^{-2}$ K min^{-1} are as follows: $T_1 = 156.6 \pm 0.2$ K and $T_2 = 174.3 \pm 0.2$ K. Some discrepancy between the values of T_1 and T_2 obtained from the calorimetric and optical experiments can be explained by the different methods used for the preparation of the samples. As was noted above, the phase transition temperatures obtained in the measurements of the dependence $\Delta n_c(T)$ differ not only for the crystals prepared by the different methods but also for both the untreated samples and the samples subjected to mechanical treatment. As was also mentioned above, for the measurements of the heat capacity $C_p(T)$, the samples were prepared by pressing ($p \approx 0.1$ GPa) of the powder obtained by grinding small single crystals of $(NH_4)_2TaF_7$.
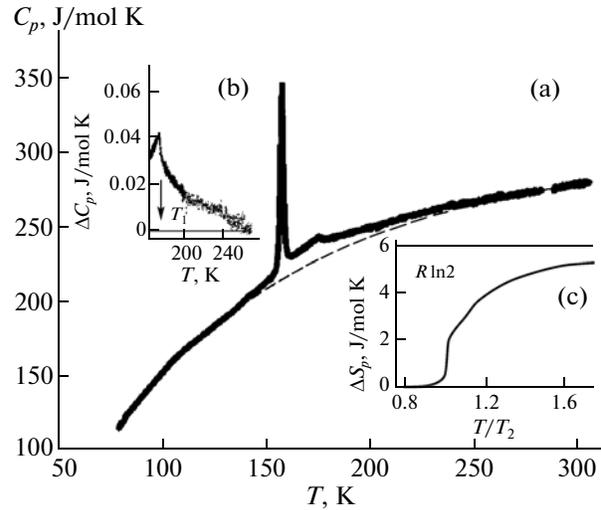

Fig. 5. Temperature dependences of (a) the molar heat capacity, (b) the anomalous heat capacity in the range of T_1, and (c) the entropy associated with the sequence of structural transformations. The dashed line shows the lattice heat capacity.

In order to obtain information on the integral thermophysical characteristics of the phase transitions, it was necessary to separate the regular and anomalous contributions to the total heat capacity of the crystal. The lattice heat capacity C_L (Fig. 5a) was determined by the approximation of the experimental data outside the region of the existence of anomalies by using, first, a combination of the Debye function $C_D(\Theta_D/T)$ and the Einstein function $C_E(\Theta_E/T)$ and, second, the polynomial function. The deviations of the experimental points from the smoothed curves for both cases were approximately identical. The variation of the temperature intervals included in the fitting procedure showed that the best results correspond to the presence of the excess heat capacity $\Delta C_p(T) = C_p - C_L$ in a wide temperature range 133–270 K.

We could not determine the integral thermal effects for each of the phase transitions because of the close temperatures of the anomalies of the heat capacity. The total enthalpy change was found to be $\Sigma\Delta H = \int \Delta C_p dT = 920 \pm 70$ J mol^{-1}. The contribution from the excess heat capacity, which exists in a very wide temperature range above T_1 (Fig. 5b), to the total enthalpy change $\Sigma\Delta H$ proved to be large enough and equal to ~40%.

It should be noted that, at temperatures close to 245 K, there is a slight violation of the regular decrease in the excess heat capacity (Fig. 5b). As was shown above, the investigation of the dielectric properties in the same temperature range revealed a small peak in the dependences $\varepsilon(T)$ and $\tan\delta(T)$ (Figs. 4a, 4c). At the same time, no anomalous behavior of the birefringence in the G_1 phase was observed.
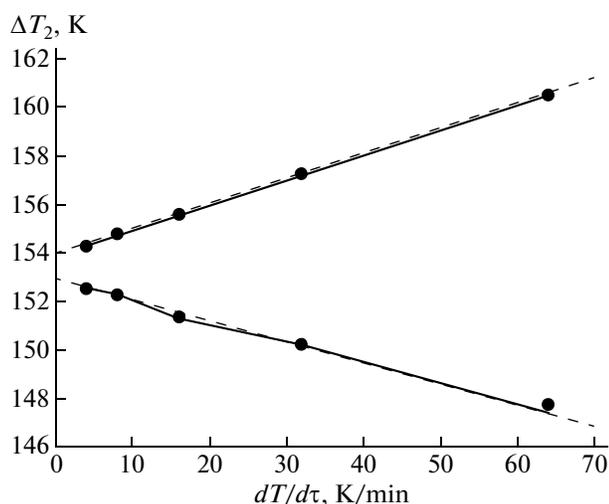
Fig. 6. Dependence of the hysteresis of the temperature T_2 on the scanning rate.

Fig. 7. Temperature dependences of (a) the coefficient of linear thermal expansion and (b) the linear deformation. The dashed line shows the lattice contribution.

The temperature dependence of the anomalous entropy $\Delta S(T)$ is shown in Fig. 5c. In accordance with the first-order phase transition, the abrupt change in ΔS at the temperature T_2 was interpreted as the entropy jump $\delta S_2 = 1.6$ J (mol K)$^{-1}$. The total entropy change associated with the sequence of phase transitions was $\Sigma\Delta S = \int(\Delta C_p/T)dT = 5.8 \pm 0.4$ J (mol K)$^{-1}$.

In the region of the first-order phase transition, the hysteresis phenomena were thoroughly investigated using differential scanning microcalorimetry and adiabatic calorimetry. For this purpose, in the first case, the values of the phase transition temperature were determined in the heating (T_2') and cooling (T_2'') modes at the scanning rates varied over a wide range: $dT/d\tau = (4-64)$ K min^{-1}. Figure 6 demonstrates a significant dependence of the phase transition temperature on the rates of heating and cooling. By extrapolating the temperatures T_2' and T_2'' to $dT/d\tau = 0$, we determined the hysteresis $\delta T_2 \approx 1$ K, which corresponds to the phase transition under quasi-equilibrium conditions. In the experiments on the adiabatic calorimeter, where the scanning rates did not exceed $dT/d\tau = 3.5 \times 10^{-2}$ K min^{-1}, the value of the hysteresis $\delta T_2 \approx 0.5$ K was found to be almost the same as in the measurements of the birefringence in the thermostating mode.

6. THERMAL EXPANSION

The thermal expansion of the $(NH_4)_2TaF_7$ crystal was investigated on a NETZSCH DIL-402C dilatometer at temperatures in the range from 90 to 320 K in the dynamic mode at the rates of change in the temperature from 2 to 4 K/min. The measurements were performed i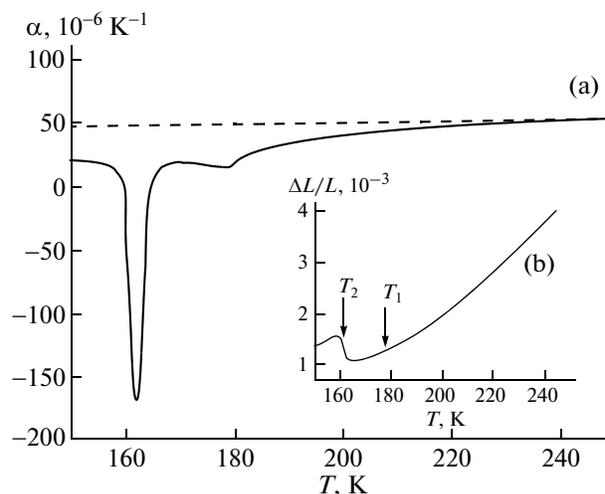n a helium flow. The calibration and the inclusion of the expansion of the measurement system were made using reference samples prepared from corundum. The dilatometric experiments were carried out with the same sample as was used in the calorimetric studies. There was good agreement between the results obtained in several series of measurements.

The temperature dependences of the linear deformation $\Delta L/L_0$ and the linear thermal expansion coefficient α measured in the heating mode are shown in Fig. 7. The temperatures of the minima of the linear thermal expansion coefficient, which were taken as the phase transition temperatures $T_1 = 157 \pm 1$ K and $T_2 = 173.8 \pm 1$ K, are in satisfactory agreement with the temperatures determined from the calorimetric measurements. It can be seen from this figure that the linear thermal expansion coefficient α is characterized by the anomalous behavior over a wide temperature range, as well as the heat capacity (Fig. 5). In order to refine the interval of the existence of the anomalous thermal expansion coefficient $\Delta\alpha$, we used the relationship between the regular components of the thermal expansion and the heat capacity in terms the law of corresponding states [14]. In the tetragonal phase $P4/nmm$ at temperatures in the range from 270 to 305 K, the relationship between these two quantities is satisfactorily described by the equation $\alpha_L(T) = KC_L(T)$ with $K = 5.85 \times 10^{-5}$ mol J^{-1}. Using the Debye and Einstein temperatures determined in the analysis of the lattice heat capacity, we restored the behavior of the lattice contribution to the thermal expansion coefficient $\alpha(T)$. As a result, it was found that, at temperatures below T_2, the anomalous thermal expansion coefficient $\Delta\alpha$ exists in a wider temperature range as compared to the excess heat capacity ΔC_p, or, more precisely, up to 100 K.

By interpreting the change in the thermal expansion coefficient $\delta\alpha = -2.9 \times 10^{-5}$ K^{-1} at the temperature T_1 as a jump associated with the second-order transition, we can draw a correlation with the jump of the heat capacity $(\delta C_p)_{T = T_1} = 15$ J (mol K)$^{-1}$ in terms of the Ehrenfest equation [14]. In order to estimate the susceptibility of the $(NH_4)_2TaF_7$ ceramic sample to hydrostatic pressure, we assumed the following relationship between the volume and linear expansion coefficients $\beta = 3\alpha$. In this case, the pressure coefficient was found to be $dT_1/dp = VT_1(\delta\alpha/\delta C_p) \approx -110$ K GPa^{-1}.

It can be seen from Fig. 6b that the linear deformation and, accordingly, the volume deformation $\Delta V/V_0 = 3\Delta L/L_0$ increase with increasing temperature, except for the region of the phase transition at the temperature T_2, where the volume drastically decreases. According to the Clapeyron−Clausius equation $dT_2/dp = (\delta V_2/V_0)/\delta S_2$ [14], the negative volume change $\delta V_2/V_0 = -1.7 \times 10^{-3}$ indicates a decrease in the temperature of the phase transition at T_2 with an increase in the hydrostatic pressure. The calculation of the quantity $dT_2/dp = -113$ K GPa^{-1} shows that the susceptibility of the temperatures of both phase transitions in $(NH_4)_2TaF_7$ to the pressure is almost identical.

The significant values of the pressure coefficients, from our point of view, can explain the aforementioned difference in the phase transition temperatures. The samples used in different experiments, to a greater or lesser extent, were subjected to external mechanical impacts associated with the operations of grinding, polishing, and pressing, which will undoubtedly lead to the emergence of different degrees of stress in these samples. Furthermore, even in the samples prepared by different methods and not subjected to mechanical treatment, the values of T_2 could differ from each other.

7. CONCLUSIONS

Thus, it has been found that, upon the substitution of the molecular cation for the atomic cation, the symmetry of the parent structure of the ammonium fluoride $(NH_4)_2TaF_7$ with a seven-coordinated anion polyhedron remains tetragonal ($P4/nmm$, $Z = 2$) with the unit cell parameters close to the parameters of the related compound Rb_2TaF_7 [7]. In this case, the temperature T_1 characterizing the stability of the phase $P4/nmm$ increases by ~30 K. During cooling, both compounds undergo a transition to the orthorhombic phase. However, the calorimetric, dilatometric, dielectric, and optical investigations have demonstrated that, in contrast to Rb_2TaF_7, this phase in the $(NH_4)_2TaF_7$ fluoride exists in a narrow temperature ($T_1 - T_2 \approx 20$ K). At temperatures below T_2, the ammonium crystal again becomes optically uniaxial

and undergoes a first-order transition to the tetragonal phase. In accordance with the character of the optical twinning and the behavior of dielectric properties, the structural distortions have a ferroelastic nature, which, most likely, determines the observed significant susceptibility of the ammonium tantalate to hydrostatic pressure.

The total entropy change associated with the sequence of phase transitions in $(NH_4)_2TaF_7$ proved to be rather large $\Sigma\Delta S \approx R\ln 2$. Since the intermediate orthorhombic phase exists in a very narrow temperature range, we could not separate the contributions to $\Sigma\Delta S$ from each of the two transitions. At the same time, the anomalous entropy is observed in a very wide temperature range, especially in the parent tetragonal phase ~$(T_1 + 90$ K$)$. This behavior of ΔS is characteristic of crystalline systems in which the correlation effects are developed to a large extent due to the absence of strong long-range forces. The possible models of distortions of the crystal unit cell cannot be adequately analyzed together with the entropy parameters of the phase transition because of the lack of detailed information on the structures of all the phases.

According to the data on the structure of the related fluorides Rb_2TaF_7 and K_2TaF_7, the seven-coordinated polyhedra $[TaF_7]^{2-}$, i.e., monocapped trigonal prisms, are disordered over two orientations due to the rotations around the local fourfold axis [4, 7]. A complete ordering of polyhedra in these fluorides due to the phase transition could be accompanied by the entropy change $R\ln 2$ corresponding to the value of $\Sigma\Delta S$ in $(NH_4)_2TaF_7$. However, there is information about the phase transition only for Rb_2TaF_7 [7], whereas data on the entropy are lacking.

Of course, the substitution Rb $\longrightarrow$ (NH_4) could lead to another character of the disordering of structural elements, including the univalent cation−ammonium tetrahedron, as is indicated, in particular, by the change in the type of the unit cell of the orthorhombic phase from base-centered to primitive, as well as by the occurrence of the second phase transition. From the above it follows that, for the understanding of the mechanism of structural distortions in A_2TaF_7 fluorides, it is of interest to perform detailed investigations of the crystal structure of all the phases of $(NH_4)_2TaF_7$ and thermophysical properties of Rb_2TaF_7.

REFERENCES

1. K. S. Aleksandrov and B. V. Beznosikov, *Perovskite-Like Crystals* (Nauka, Novosibirsk, 1997) [in Russian].

2. K. S. Aleksandrov and B. V. Beznosikov, *Perovskites: Present and Future* (Siberian Branch of the Russian Academy of Sciences, Novosibirsk, 2004) [in Russian].

3. I. N. Flerov, M. V. Gorev, K. S. Aleksandrov, A. Tressaud, J. Grannec, and M. Couzi, Mater. Sci. Eng., R **24**, 81 (1998).

4. E. C. Reynhardtt, J. C. Pratt, A. Watton, and H. E. Petch, J. Phys. C: Solid State Phys. **14**, 4701 (1981).

5. H. J. Hurst and J. C. Taylor, Acta Crystallogr., Sect. B: Struct. Crystallogr. Cryst. Chem. **26**, 417 (1970).

6. T. Buni, M. Tramsek, E. Goreshnik, and B. Zemva, Solid State Sci. **9**, 88 (2007).

7. N. M. Laptash, A. A. Udovenko, and T. B. Emelina, J. Fluorine Chem. **132**, 1152 (2011).

8. S. V. Misyul, S. V. Mel'nikova, A. F. Bovina, and N. M. Laptash, Phys. Solid State **50** (10), 1951 (2008).

9. M. C. Marignac, Ann. Chim. Phys. **9**, 249 (1866).

10. I. N. Flerov, M. V. Gorev, S. V. Mel'nikova, S. V. Misyul', V. N. Voronov, K. S. Aleksandrov, A. Tressaud, J. Grannec, J.-P. Chaminade, L. Rabardel, and H. Faget-Guengard, Phys. Solid State **34** (11), 1870 (1992).

11. I. N. Flerov, V. D. Fokina, A. F. Bovina, E. V. Bogdanov, M. S. Molokeev, A. G. Kocharova, E. I. Pogorel'tsev, and N. M Laptash, Phys. Solid State **50** (3), 515 (2008).

12. A. Guyomar, G. Sebald, B. Guihard, and L. Seveyrat, J. Phys. D: Appl. Phys. **39**, 4491 (2006).

13. V. S. Bondarev, A. V. Kartashev, A. G. Kozlov, I. Ya. Makievskii, I. N. Flerov, and M. V. Gorev, Preprint No. 829F, IF SO RAN (Kirensky Institute of Physics, Siberian Branch of the Russian Academy of Sciences, Krasnoyarsk, 2005).

14. L. D. Landau and E. M. Lifshitz, *Course of Theoretical Physics*, Vol. 5: *Statistical Physics: Part 1* (Nauka, Moscow, 1964; Butterworth−Heinemann, Oxford, 1968).

Translated by O. Borovik-Romanova